

Structural Elucidation of Biological and Toxicological Complexes: Investigation of Monomeric and Dimeric Complexes of Histidine with Multiply Charged Transition Metal (Zn and Cd) Cations using IR Action Spectroscopy

Theresa E. Hofstetter,[†] Collin Howder,[‡] Giel Berden,[§] Jos Oomens,^{§,||} and P. B. Armentrout*,[†]

[†]Department of Chemistry, University of Utah, 315 S. 1400 E. Rm 2020, Salt Lake City, Utah 84112, United States

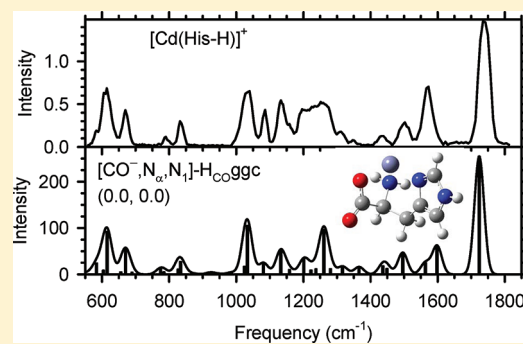
[‡]Department of Biology and Chemistry, Spring Arbor University, 106 E. Main St., Spring Arbor, Michigan 49283, United States

[§]FOM Institute for Plasma Physics Rijnhuizen, Edisonbaan 14, NL-3439 MN Nieuwegein, The Netherlands

^{||}van't Hoff Institute for Molecular Sciences, University of Amsterdam, Science Park 904, 1098 XH Amsterdam, The Netherlands

 Supporting Information

ABSTRACT: The gas-phase structures of singly and doubly charged complexes involving transition metal cations, Zn and Cd, bound to the amino acid histidine (His) as well as deprotonated His (His-H) are investigated using infrared multiple photon dissociation (IRMPD) spectroscopy utilizing light generated by a free electron laser. IRPMD spectra are measured for CdCl⁺(His), [Zn(His-H)]⁺, [Cd(His-H)]⁺, Zn²⁺(His)₂, and Cd²⁺(His)₂ in the 550–1800 cm⁻¹ range. These studies are complemented by quantum mechanical calculations of the predicted linear absorption spectra at the B3LYP/6-311+G(d,p) and B3LYP/Def2TZVP levels. The monomeric spectra are similar to one another and indicate that histidine coordinates to the metal in a charge-solvated (CS) tridentate form in the CdCl⁺(His) complex and has a similar tridentate configuration with a deprotonated carboxylic acid terminus in the [M(His-H)]⁺ complexes. The preference for these particular complexes is also found in the relative energetics calculated at the B3LYP, B3P86, and MP2(full) levels. The spectra of the dimer complexes have obvious CS characteristics, suggesting that at least one of the His ligands is charge solvated; however, there are also signatures for a salt-bridge (SB) formation in the second His ligand. The definitive assignment of a SB ligand is complicated by the presence of the CS ligand and conflicting relative energetics from the different levels of theory.



INTRODUCTION

Under physiological conditions, zinc exists as the divalent Zn²⁺ cation and plays a significant role as the metal center of carbonic anhydrase, a metalloenzyme with three histidine (His) residues coordinated to a zinc ion, and in the zinc finger protein.^{1–6} The zinc finger protein module is abundant in all mammalian genes and is responsible for DNA- and RNA-binding, cell cycle signaling, and protein–protein interactions.⁴ The classic binding motif of the zinc finger has Zn²⁺ directly coordinated to two His and two cysteine (Cys) residues,¹ but Zn²⁺(His)(Cys)₃ formation has also been identified. Both motifs are associated with proteins that recognize, bind, and repair DNA and RNA.^{5,7} The zinc finger is a sensitive target for toxic heavy metals like Cd²⁺ because the zinc ion can be replaced by even low concentrations of certain metals, thereby inhibiting the functionality of the zinc-dependent complex.⁸ This inactivation has a profound effect on genomic stability, the reproductive system, brain development, and may increase the risk of tumor development.^{7,8} Because cadmium can bioaccumulate and anthropomorphic emissions into the environment are 18 times higher than naturally occurring rates, human

and environmental exposure to this metal is a major threat.^{8–10} In contrast to the zinc finger proteins, it has been suggested that the carbonic anhydrase metalloenzyme may not be completely deactivated by replacement of Zn²⁺ with Cd²⁺.¹¹

Using a variety of condensed phase experimental techniques for structural determination (e.g., crystallography, NMR), the mechanism for protein inactivation by removal of the zinc is presumed to be structural changes or chemical modification (oxidation) of the coordinating residues.^{1–5,7,8,12} These proposed mechanisms of deactivation are influenced by varying protein structures, protein interactions, and solvent. Studying these complexes in isolation may be beneficial to better understand the modifications of the coordinating residues upon metal substitution.

One strategy for investigating the fundamental interactions between a metal and its metal-site in a protein is to study these

Received: July 30, 2011

Revised: September 16, 2011

Published: September 20, 2011

metals coordinated to the pertinent chelating residues in the gas-phase, creating a biomimetic complex. This approach has been used for monomeric, dimeric, and trimeric complexes of histidine and similar molecules like aromatic amino acids, tryptophan (Trp) and phenylalanine (Phe), with singly and doubly charged metal cations as well as in protonated dipeptides and complexed with variety of singly charged anions.^{13–25} Here, we have undertaken a systematic conformational investigation of zinc and cadmium binding one and two His residues using infrared multiple photon dissociation (IRMPD) action spectroscopy and quantum chemical calculations.

As mentioned above, physiologically relevant complexes have both one and two His coordinated directly to Zn^{2+} . Hence IRMPD spectra were obtained for $M^{2+}(His)_2$, where $M = Zn$ and Cd. The doubly charged monomeric complexes, $M^{2+}(His)$, were not formed experimentally, but the spectra of deprotonated His with both metals, $[M(His-H)]^+$, were also measured. To see whether deprotonation affects the structure, the spectrum of the $CdCl^+(His)$ complex was also measured. Conformations are identified by comparing experimental spectra to single photon spectra predicted by quantum chemical calculations of low-energy structures calculated at the B3LYP/6-311+G(d,p) level for Zn^{2+} complexes and B3LYP/Def2TZVP for Cd^{2+} complexes. Relative energies for these complexes are calculated using B3LYP, B3P86, and MP2(full) levels with the 6-311+G(2d,2p) basis set for Zn^{2+} complexes and Def2TZVPP basis set for Cd^{2+} complexes. Structural elucidation of these complexes will lead to fundamental understanding of the effect of the metal on such a biologically important binding site.

■ EXPERIMENTAL AND THEORETICAL METHODS

Mass Spectrometry and IRMPD Spectroscopy. A 4.7 T Fourier transform ion cyclotron resonance (FT-ICR) mass spectrometer^{14,26,27} coupled to a beamline of the free electron laser for infrared experiments (FELIX)²⁸ was used to record the IRMPD spectra. Reactant ion complexes were formed by electrospray ionization (ESI) using a Micromass Z-spray source and a solution of 1 mM zinc nitrate (or cadmium chloride) and 1 mM His in 50:50 MeOH:H₂O solution with a solution flow rate of ~10 μ L/min. All chemicals were obtained from Aldrich. Ions were accumulated in a hexapole trap for ~4 s prior to being pulse injected into the ICR cell via an rf octopole ion guide. Before entering the ICR cell, ions are decelerated out of the octopole in such a way that they can be captured without a gas pulse such that collisional heating of the ions is avoided.¹⁴ Once trapped in the cell, the ion of interest is mass isolated using a stored waveform inverse Fourier transform (SWIFT) excitation pulse. Spectra were recorded over the wavelength range from 18.2 μ m (550 cm⁻¹) to as far as 5.5 μ m (1830 cm⁻¹). FELIX pulse energies were around 50 mJ/macropulse of 5 μ s duration. The ion of interest was irradiated for 3–3.5 s at 5 or 10 Hz macropulse repetition rate, which corresponds to interaction with approximately 15–18 macropulses at 5 Hz or 30–35 macropulses at 10 Hz. For all but the $[Cd(His-H)]^+$ spectrum, various intense bands in the spectra were also probed with 3 dB attenuated laser energy to avoid saturation and better represent relative intensities and peak shapes. The full width at half-maximum (fwhm) bandwidth of the laser was typically 0.5% of the central wavelength. IRMPD spectra were constructed by plotting the total ionic fragmentation yield as a function of the wavenumber of the radiation.

The ESI source generated $Zn^{2+}(His)_2$, $Cd^{2+}(His)_2$, and $CdCl^+(His)$ directly. The $[M(His-H)]^+$ species were not directly produced in the ESI source but were generated by irradiating larger ions with a 40-W continuous-wave CO₂ laser for 1 s and then allowing the resulting ions to cool for an additional 1 s before irradiation with the FELIX light. $[Zn(His-H)]^+$ was formed from $[Zn(His-H)NH_3]^+$, and $[Cd(His-H)]^+$ was formed from the $Cd^{2+}(His)_2$ species.

Quantum Chemical Calculations. Starting geometries for $Zn^{2+}(His)$ complexes were taken from geometries of $Li^+(His)$ complexes.¹⁶ Using the Gaussian 09 suite of programs,²⁹ these structures were further optimized at the B3LYP/6-31G(d) level^{30,31} using the “loose” keyword, which utilizes a large step size (0.01 au) and rms force constant (0.0017) to ensure a rapid geometry convergence followed by geometry optimization at the B3LYP/6-311+G(d,p) level. From $Zn^{2+}(His)$, the His residue was deprotonated at likely sites and the loose optimization step repeated. Unique structures remaining after this procedure were chosen for further geometry optimization and vibrational frequency calculations at the B3LYP/6-311+G(d,p) level ensuring structural convergence during the frequency calculation. The $[Zn(His-H)]^+$ and $Zn^{2+}(His)$ complexes were also used as the starting geometries for the $[Cd(His-H)]^+$ and $CdCl^+(His)$ systems, respectively. Here the same geometry optimization procedures were followed using the B3LYP/Def2TZVP level, where Def2TZVP is a size-consistent basis set for all atoms and includes triple- ζ + polarization functions with an effective core potential (ECP) on Cd having 28 electrons (small core).^{32,33} The Def2TZVP basis set and ECP were obtained from the EMSL basis set exchange.³⁴ Because of their large size and many degrees of freedom, a comprehensive structure search for the dimeric complexes was not undertaken, but low-energy binding motifs found for $Zn^{2+}(His)$ were combined to give likely complexes of $Zn^{2+}(His)_2$ and $Cd^{2+}(His)_2$. Once constructed, we performed geometry optimization and frequency calculations for these complexes similar to those described for the monomeric complexes.

For comparison to experiment, the vibrational frequencies and IR intensities were calculated using the harmonic oscillator approximation at the B3LYP level and were broadened using a 20 cm⁻¹ fwhm Gaussian line shape. Frequencies were scaled by 0.975, consistent with scaling factors found appropriate in other studies of this spectral region on similar complexes of His.^{16,19–22}

Single-point energy calculations were carried for the most stable structures at the B3LYP, B3P86,³⁵ and MP2(full)³⁶ levels using the 6-311+G(2d,2p) basis set for Zn complexes and Def2TZVPP basis set for Cd complexes. The relative energies between each isomer include zero-point energy (ZPE) corrections to yield 0 K values and thermal corrections to free energies at 298.15 K. These corrections use the calculated frequencies scaled by 0.989, a scaling factor determined by Bauschlicher and Partridge to give accurate ZPE corrections at the B3LYP level using a 6-311+G(3df,2p) basis set.³⁷

■ RESULTS AND DISCUSSION

Theoretical Results. The low-lying structures found for $CdCl^+(His)$ are shown in Figure 1 and illustrate the likely coordination modes of His to both Zn^{2+} and Cd^{2+} . The Cl⁻ is a spectator ion and has little effect on the Cd–His coordination, as also seen previously for $CdCl^+(Trp)$.¹⁹ The nomenclature used to identify different structural isomers is similar to that described previously for the IRMPD studies of other metal–amino

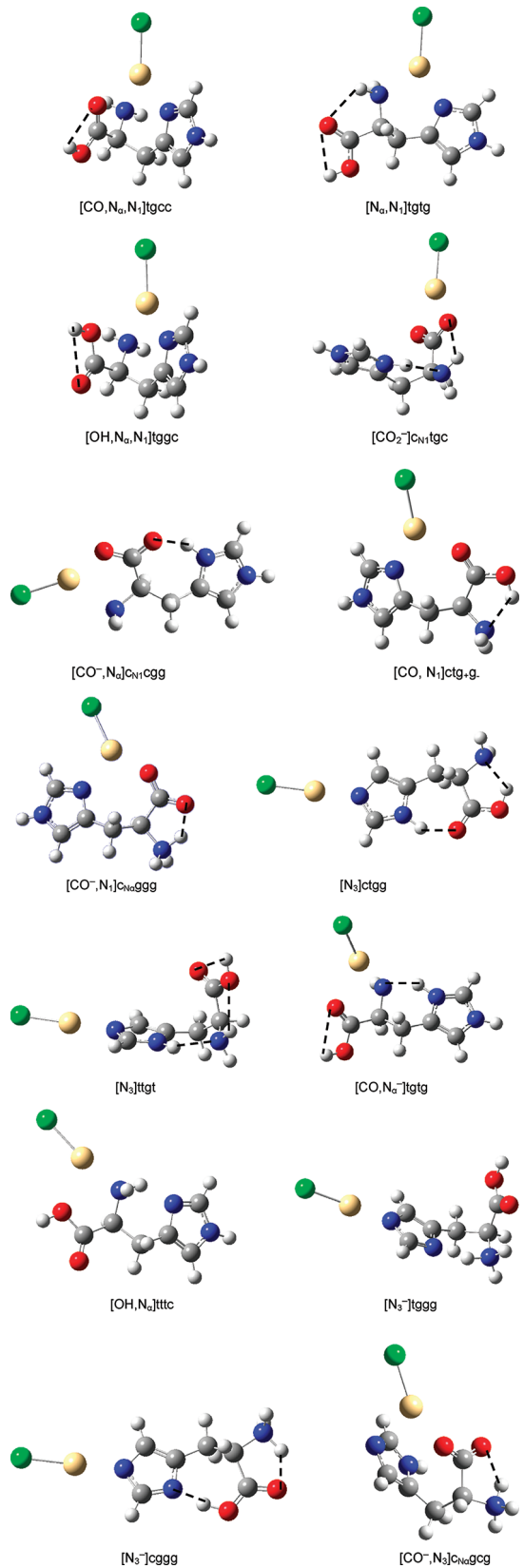


Figure 1. Structures of the $\text{CdCl}^+(\text{His})$ complexes calculated at the B3LYP/Def2TZVP level of theory. Hydrogen bonds are indicated by dashed lines.

acids.^{38–40} Briefly, conformations in this study are identified by their metal binding site in brackets, followed by a description of

the His orientation by a series of four dihedral angles. For the charge-solvated (CS) structures, these angles start with the carboxylic acid hydrogen to define the $\text{H}-\text{O}-\text{C}-\text{C}_\alpha$ angle and proceed along the molecule ending with the “pro” nitrogen (N_1 , also commonly designated as N_π) of the imidazole side chain, which is the nitrogen closest to the β -carbon of the backbone. These angles define the $\text{O}-\text{C}-\text{C}_\alpha-\text{C}_\beta$, $\text{C}-\text{C}_\alpha-\text{C}_\beta-\text{C}$, and $\text{C}_\alpha-\text{C}_\beta-\text{C}-\text{N}_1$ dihedrals and are distinguished as cis (c, for angles between 0° and 50°), gauche (g, between 50° and 135°), and trans (t, between 135° and 180°). For most salt-bridge (SB) conformations, the proton originally on the carboxylic acid is attached to either the α -amino (N_α) or N_1 nitrogens. For these complexes, the first dihedral angle starts at this bridging proton and moves along the molecule toward the deprotonated site and is labeled using a subscript according to where this proton is located (either N_α or N_1). The remaining three dihedrals are the same as above starting at the CO^- involved in the salt-bridge. Salt-bridges are also formed between the N_α and N_1 atoms, leaving the carboxylic acid group intact. These structures are higher in energy and the nomenclature remains the same as for the CS complexes, with the particular SB motif explicitly noted. In all conformations, the $\text{C}_\beta-\text{C}-\text{N}_1-\text{C}$, $\text{C}-\text{N}_1-\text{C}-\text{N}_3$ (where N_3 is the “tele” or far nitrogen in the imidazole, also designated N_π elsewhere), and $\text{N}_1-\text{C}-\text{N}_3-\text{C}$ dihedrals are consistently found to have a “tcc” designation because of the steric constraints of the imidazole ring. Thus, these orientations are omitted from our nomenclature. For the deprotonated complexes studied here, $[\text{M}(\text{His}-\text{H})]^+$, the question of CS versus SB does not arise, although there are many possible deprotonation sites from each complex. As such, the nomenclature includes a “ $-\text{H}_n$ ” designation following the coordination sites, where n defines the deprotonation site. If the deprotonation site is the NH_2 group on the α carbon, then the $\text{H}-\text{N}_\alpha-\text{C}_\alpha-\text{C}_\beta$ dihedral is given in parentheses to define the angle of the proton still remaining. The nomenclature of the dimeric complexes combines names of the monomeric complexes in a straightforward fashion.

Monomeric Species. Relative energies, including zero-point energy (ZPE) corrections with respect to the ground state (GS) calculated at three different levels of theory, are given in Table 1 for the $\text{CdCl}^+(\text{His})$ and $[\text{M}(\text{His}-\text{H})]^+$ complexes. Because the relative Gibbs free energies at 298 K may be more relevant in describing the experimental distributions, these values are also listed in Table 1 and complexes are ordered with respect to increasing 298 K free energy at the B3LYP level. Table 1 includes all likely coordination sites for the $\text{CdCl}^+(\text{His})$ system, although conformers having similar coordination sites but different dihedral angles are presented in the Supporting Information, Table S1 and Figure S1. Because of the large number of possible structures and deprotonation sites, only selected isomers are listed in Table 1 for the $[\text{M}(\text{His}-\text{H})]^+$ systems, with all structures presented in Table S1 and Figure S1 of Supporting Information.

The CS tridentate $[\text{CO}_2\text{N}_\alpha\text{N}_1]\text{tgcc}$ structure is the lowest energy conformation for $\text{CdCl}^+(\text{His})$ at all three levels of theory. This structure is similar to the CS1 conformation reported as the GS configuration by Dunbar and co-workers in their study of Ba^{2+} –(His) and Ca^{2+} –(His).¹⁵ Other CS conformations with $[\text{N}_\alpha\text{N}_1]$ and $[\text{OH},\text{N}_\alpha,\text{N}_1]$ coordination sites are 16–26 kJ/mol higher in 298 K free energy than the GS (Table 1). The lowest energy SB structures reported previously¹⁵ for Ca^{2+} and Ba^{2+} have $[\text{CO}_2^-]$ and $[\text{CO}^-, \text{N}_\alpha]$ coordination sites (Figure 1). Interestingly these structures are 30–34 kJ/mol higher in 298 K free energy at the density functional theory (DFT) levels but are predicted to be

Table 1. Relative Enthalpy at 0 K (ΔH_0) and Free Energies at 298 K (ΔG_{298}^a) (kJ/mol) of Low-Lying Conformers of Cationized Monomeric His and His-H^b

complex	structure	B3LYP	B3P86	MP2(full)
CdCl ⁺ (His)	[CO,N _α N ₁]tgcc	0.0 (0.0)	0.0 (0.0)	0.0 (0.0)
	[N _α N ₁]tgtg	19.8 (15.9)	22.6 (18.7)	30.2 (26.3)
	[OH,N _α N ₁]tggc	24.6 (22.4)	26.6 (24.5)	22.6 (20.5)
	[CO ₂ ⁻]c _{N1} tgc	34.8 (29.6)	39.0 (33.8)	63.5 (58.3)
	[CO ⁻ ,N _α]c _{N1} cgg	32.3 (31.0)	34.4 (33.0)	64.9 (63.5)
	[CO,N ₁]ctg,g-	41.2 (37.9)	43.9 (40.6)	61.6 (58.4)
	[CO ⁻ ,N ₁]c _{Nα} ggg	64.6 (60.9)	64.9 (61.2)	80.4 (76.8)
	[N ₃]ctgg	70.0 (68.2)	73.3 (71.5)	95.0 (93.2)
	[N ₃]tgtt	73.1 (68.9)	79.9 (75.6)	89.8 (85.6)
	[CO,N _α ⁻]tgtg ^c	86.1 (84.4)	85.4 (83.7)	105.7 (104.0)
	[OH,N _α]tttc ^c	88.0 (84.8)	92.1 (88.9)	103.1 (99.9)
	[N ₃ ⁻]tggg ^c	88.2 (85.4)	89.1 (86.3)	95.0 (92.2)
	[N ₃ ⁻]cggg ^d	113.0 (111.6)	109.6 (108.2)	125.8 (124.4)
	[CO ⁻ ,N ₃]c _{Nα} g _c	154.1 (150.5)	156.0 (152.4)	155.1 (151.5)
[Cd(His-H)] ⁺	[CO ⁻ ,N _α N ₁]-H _{CO} ggc	0.0 (0.0)	0.0 (0.0)	0.0 (0.0)
	[CO,N _α ⁻ ,N ₁]-H _{Nα} (t)tgcc	24.7 (24.2)	26.2 (25.7)	29.6 (29.2)
	[CO,N _α ⁻ ,N ₁]-H _{Nα} (c)tgcc	38.3 (37.8)	38.9 (38.4)	39.0 (38.5)
	[CO,N _α N ₁]-H _{N3} tgcc	80.0 (79.6)	80.2 (79.8)	73.3 (72.9)
	[N ₃]-H _{Nα} (t)ttgg	272.0 (261.2)	301.0 (290.2)	27.9 (17.2)
	[N ₃]-H _{Nα} (c)ctgg	282.4 (273.2)	309.5 (300.3)	25.4 (16.2)
	[CO ⁻ ,N _α N ₁]-H _{CO} ggc	0.0 (0.0)	0.0 (0.0)	0.0 (0.0)
[Zn(His-H)] ⁺	[CO,N _α ⁻ ,N ₁]-H _{Nα} (t)tgcc	43.8 (43.7)	44.9 (44.7)	48.2 (48.0)
	[CO,N _α ⁻ ,N ₁]-H _{Nα} (c)tgcc	54.0 (53.9)	53.7 (53.6)	53.9 (53.8)
	[CO,N _α N ₁]-H _{N3} tgcc	102.0 (102.1)	101.4 (101.5)	98.8 (98.9)
	[N ₃]-H _{Nα} (t)ttgc	379.8 (369.7)	410.8 (400.6)	108.6 (98.4)
	[N ₃]-H _{Nα} (t)cggg	385.0 (377.0)	416.0 (408.0)	170.7 (162.8)

^a ΔG_{298} values are given in parentheses. ^b Values are single-point energies calculated at the level shown using a 6-311+G(2d,2p) basis set for Zn-containing complexes and Def2TZVPP for Cd-containing complexes. Geometries are calculated at the B3LYP/6-311+G(d,p) level for Zn-containing complexes and B3LYP/Def2TZVP for Cd-containing complexes. Zero-point energy corrections scaled by 0.989 are included. ^c Salt-bridge between N_α and N₁. ^d Salt-bridge between the N_αH₃⁺, COOH, and N₁⁻ groups.

58–64 kJ/mol higher than the GS at the MP2(full) level. On the basis of the trends seen in Table 1, the MP2(full) level favors CS complexes and predicts SB structures to be much higher in energy compared to the predicted relative energetics of the same structures at the DFT levels. Previous work has found that the CS structures of M²⁺(Trp) are highly stable for small, doubly charged metals, like Cd and Zn.²² However, contributions from SB structures cannot be ruled out by relative energetics alone, as calculations tend to overestimate the stability of the CS structures versus SB conformers of M²⁺(His) as determined on the basis of spectral assignments.¹⁵

The higher energy complexes given in the Supporting Information include several [CO,N₁] conformers, where each one differs slightly in the orientation of the amino acid such that the direction of the gauche dihedral angles must also be specified (either + or -). The lowest of these is included in Figure 1 and Table 1. Each structure is predicted to be 38–60 kJ/mol above the GS and to have fairly similar vibrational frequencies, although the position and relative intensity of the COH bend is dependent on the orientation of the hydroxyl and α-amino groups, as seen in the Supporting Information. The [CO,N_α⁻]tgtg complex is the lowest energy SB structure in which the proton bridges N_α and N₁ (Figure 1), but it is still 46–55 kJ/mol higher in 298 K free energy than the [CO₂⁻] SB complex. The [N₃]ctgg and [N₃]tgtt

complexes have similar metal coordination and extended configurations, but they differ in the orientation of the α-amino and carboxylic acid groups and resulting intermolecular H-bonding. In [N₃]ctgg, the proton on the hydroxyl H-bonds with the NH₂ group, while the proton on N₁ H-bonds to the carbonyl group. In [N₃]tgtt, the NH₂ group accepts a H-bond from the proton on the N₁, while the hydroxyl oxygen H-bonds with the NH₂ group. These changes result in free energy differences of $\Delta\Delta G_{298} = -7.6$ to 4.1 kJ/mol. Similar differences are seen in the intramolecular binding of the amino acid between the two extended SB structures, [N₃⁻]tgcc and [N₃⁻]cgcc. In the former, the NH₃⁺ group H-bonds to both the N₁ of the imidazole ring and the carbonyl oxygen, whereas in the [N₃⁻]cgcc complex, the NH₃⁺ H-bonds to the carbonyl and the hydroxyl H-bonds to the N₁ atom (Figure 1). As such, in the latter structure two H-bonds are used to form a salt-bridge between three groups: N_αH₃⁺, COOH, and N₁⁻. The highest energy structure located is a SB with the metal coordinated to both “ends” of the amino acid in a [CO⁻,N₃] fashion and is 150–153 kJ/mol higher than the GS structure.

For the deprotonated [M(His-H)]⁺ species, the lowest-energy structure for both the Zn and Cd systems corresponds to a tridentate GS, [CO⁻,N_αN₁], with a deprotonated carboxylic acid terminus (Table 1). This is in agreement with previous

Table 2. Relative Enthalpy at 0 K (ΔH_0) and Free Energies at 298 K (ΔG_{298}^a) (kJ/mol) of Low-Lying Conformers of Cationized Dimeric His^b

complex	structure	B3LYP	B3P86	MP2(full)
$Zn^{2+}(His)_2$	$[CO,N_\alpha,N_1]tggc/[CO^-,N_\alpha]c_{N1}cgg$	0.0 (0.0)	0.0 (0.0)	31.3 (26.0)
	$[CO,N_\alpha,N_1]tggc/[CO_2^-]c_{N1}tgc$	6.6 (1.8)	7.8 (3.0)	41.8 (31.7)
	$[CO,N_\alpha,N_1]tggc/[CO^-]c_{N1}tgc$	10.0 (8.9)	13.1 (12.0)	46.2 (39.9)
	$[CO^-,N_\alpha]c_{N1}cgg/[CO^-,N_\alpha]c_{N1}cgg$	10.2 (10.2)	13.8 (13.8)	73.3 (68.0)
	$[CO,N_\alpha,N_1]tgcc/[CO,N_\alpha,N_1]tgcc$	5.5 (10.8)	6.2 (11.5)	0.0 (0.0)
	$[CO,N_\alpha,N_1]tgcc/[CO,N_\alpha]ctgg$	14.7 (17.7)	14.4 (17.4)	30.2 (27.9)
	$[CO,N_\alpha,N_1]tgcc/[CO_2^-]t_{N1}tgc$	4.1 (0.0)	6.2 (0.0)	42.5 (31.9)
$Cd^{2+}(His)_2$	$[CO,N_\alpha,N_1]tgcc/[CO,N_\alpha,N_1]tgcc$	0.0 (6.5)	0.0 (4.4)	0.0 (0.0)
	$[CO,N_\alpha,N_1]tgcc/[CO^-,N_\alpha]c_{N1}cgg$	8.8 (8.9)	9.3 (7.3)	46.7 (40.2)
	$[CO,N_\alpha,N_1]tgcc/[CO_2^-]c_{N1}cgg$	21.5 (15.5)	26.6 (18.6)	65.1 (52.6)
	$[CO,N_\alpha,N_1]tgcc/[CO,N_1]ctgg$	20.2 (21.7)	20.3 (19.6)	41.3 (36.2)
	$[CO^-,N_\alpha]c_{N1}cgc/[CO^-,N_\alpha]c_{N1}cgc$	22.7 (22.1)	25.9 (23.2)	92.0 (84.8)

^a ΔG_{298} values are given in parentheses. ^b Values are single-point energies calculated at the level shown using the 6-311+G(2d,2p) basis set for Zn-containing complexes and Def2TZVPP for Cd-containing complexes. Geometries are calculated at the B3LYP/6-311+G(d,p) level for Zn-containing complexes and B3LYP/Def2TZVP for Cd-containing complexes. Zero-point energy corrections scaled by 0.989 are included.

work on $[Zn(Phe)(Phe-H)]^+$, which found a similar deprotonation and coordination of Phe-H.¹⁴ Both Zn and Cd form a $[CO^-,N_\alpha,N_1]$ -H_{CO}g_c configuration, which is predicted as the GS for all three levels of theory. This structure is similar to $[CO,N_\alpha,N_1]tgcc$ of Figure 1 without the hydroxyl oxygen. Deprotonation is also possible from the N_α and N₃ sites. Deprotonation of either of the two hydrogens on the α-amino group form the next higher-energy complexes, $[CO,N_\alpha,N_1^-]-H_{N\alpha}(t)tgcc$ and $[CO,N_\alpha,N_1^-]-H_{N\alpha}(c)tgcc$ for $[M(His-H)]^+$, although the latter complex differs slightly in the dihedral angles for Zn. The former structure is 24–29 (44–48) kJ/mol higher in 298 K free energy than the GS for Cd (Zn), and the latter structure is another 9–14 (6–10) kJ/mol higher. The two structures are differentiated by the H_{Nα}(t) or (c) dihedral, where the t orientation allows this proton to point toward the oxygen of the carbonyl, whereas in the less stable c orientation, it points away. Deprotonation of N₃ in the imidazole ring results in a Cd $[CO,N_\alpha,N_1^-]-H_{N3}tggg$ ($Zn[CO,N_\alpha,N_1^-]-H_{N3}tgcc$) configuration that is 73–80 (99–102) kJ/mol in 298 K free energy than the GS complex (Table 1).

Relative energetics of higher energy structures for the remaining coordination sites are given in the Supporting Information, although these complexes are >40 kJ/mol for both systems at all levels of theory. Interestingly, there are two extended structures calculated for both metal systems, where the predicted relative energetics between the DFT and MP2(full) levels are in especially poor agreement and therefore are included in Table 1. For both systems, the $[N_3^-]-H_{N\alpha}(t)ttgg$ and $[N_3^-]-H_{N\alpha}(c)ctgg$ complexes are very high in energy at the DFT levels $\Delta\Delta G_{298K} = 261$ – 300 (370–408) kJ/mol, but they are only 16–17 (98–163) kJ/mol higher than the GS at the MP2(full) level. These structures differ in the orientation of the α-amino group similar to the $[N_3^-]$ complexes described above for the CdCl⁺-(His) system. Briefly, in the $[N_3^-]-H_{N\alpha}(t)ttgg$ complex, the H_{Nα}[−] group accepts a H-bond from the N₁ group, while donating a H-bond to the hydroxyl oxygen. In the $[N_3^-]-H_{N\alpha}(c)ctgg$ complex, H_{Nα}[−] accepts a H-bond from the hydroxyl group and N₁H H-bonds to the carbonyl. The discrepancy between the predictions of different levels of theory of these complexed amino acids obviously extends further than just the CS versus SB question.

Dimeric Species. Relative energies including ZPE with respect to the GS are given in Table 2 for the $Zn^{2+}(His)_2$ and $Cd^{2+}(His)_2$ complexes. Structures of the $Zn^{2+}(His)_2$ complexes are shown in Figure 2. Relative energies and structures of higher-energy complexes are given in the Supporting Information, Table S2 and Figure S2. The majority of the low-energy structures have one charge-solvated His with a $[CO,N_\alpha,N_1]$ coordination. In the $Zn^{2+}(His)_2$ system, the lowest-energy structure at the DFT levels is a $[CO,N_\alpha,N_1]tggc/[CO^-,N_\alpha]c_{N1}cgg$ complex, where the second His ligand is in a SB conformation (Figure 2). At the MP2(full) level, this complex is fairly high in 298 K free energy ($\Delta\Delta G_{298K} = 26.0$ kJ/mol) because SB configurations are disfavored by this level of theory, as discussed above.

Disagreements between the levels of theory are also seen for the next two low-energy complexes, which involve the binding of CS and SB structures (Table 2). The $[CO,N_\alpha,N_1]tggc/[CO_2^-]c_{N1}tgc$ is only 2–3 kJ/mol above the GS in 298 K free energy at the DFT levels, but this increases to 32 kJ/mol at the MP2(full) level (6 kJ/mol above the lowest CS/SB structure). On the second His, the zinc is coordinated to the carboxylate group with Zn–O distances of 2.099 and 2.139 Å. Similar to this structure is the tetrahedral coordination of the $[CO,N_\alpha,N_1]tggc/[CO^-]c_{N1}tgc$ complex. On the SB His, the zinc dication is coordinated mainly to one oxygen of the carboxylate instead of the entire CO₂[−] group with Zn–O distances of 1.909 and 2.774 Å. This four-coordinate structure is higher in energy than the respective GSs by 9–12 kJ/mol at the DFT levels and 40 kJ/mol at the MP2(full) level (14 kJ/mol above the lowest CS/SB structure). Slightly above this complex in energy at the DFT levels is a SB/SB complex with C₂ symmetry, $[CO^-,N_\alpha]c_{N1}cgg/[CO^-,N_\alpha]c_{N1}cgg$, although because both ligands have a SB formation this particular configuration is 68 kJ/mol higher than the MP2(full) GS (Table 2). Instead, the MP2(full) GS is also a C₂ symmetric structure, where both ligands are the charge-solvated GS discussed above, $[CO,N_\alpha,N_1]tggc/[CO,N_\alpha,N_1]tggc$ (Figure 2). The CO groups are further from the metal such that the Zn–O distances are 2.964 Å, which is an increase of 0.524 Å compared to the Zn–O distance of the carbonyl in the CS ligand in the $[CO,N_\alpha,N_1]tggc/[CO^-,N_\alpha]c_{N1}cgg$ complex. This large increase in the zinc–carbonyl coordination is most likely a result of

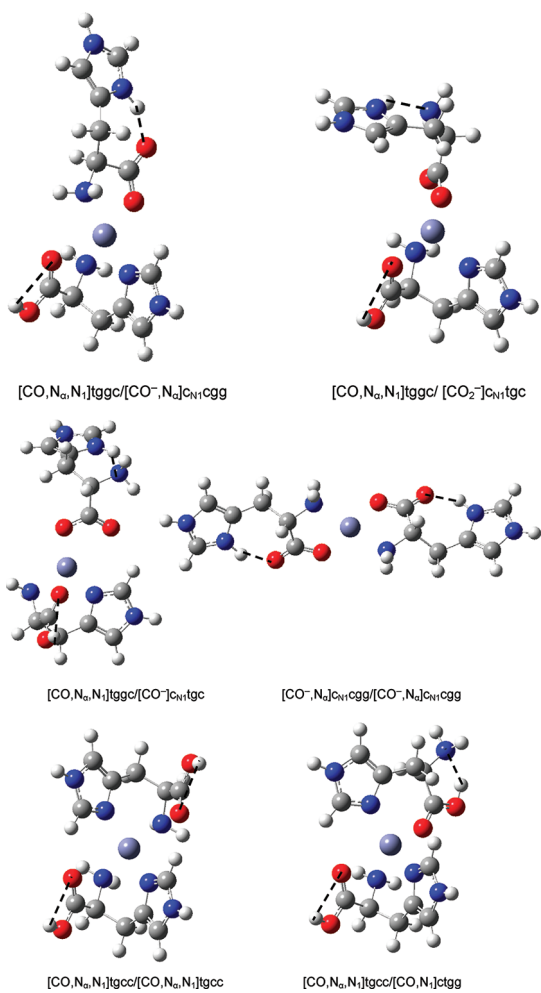


Figure 2. Low-energy structures of the $\text{Zn}^{2+}(\text{His})_2$ complexes calculated at the B3LYP/6-311+G(d,p) level of theory. Hydrogen bonds are indicated by dashed lines.

crowding and steric hindrance of the amino acid trying to coordinate six binding sites around the small zinc ion (ionic radius = 0.78 \AA^{41}) and because the carbonyl is quite close to the imidazole ring of the opposing His ligand (Figure 2).

To reduce this crowding around Zn^{2+} , we constructed a five-coordinate CS/CS complex, $[\text{CO},\text{N}_\alpha,\text{N}_1]\text{tgcc}/[\text{CO},\text{N}_1]\text{ctgg}$. In this complex, the $\text{Zn}-\text{O}$ distance to the carbonyl on the bidentate ligand is 2.066 \AA and on the tridentate His is 2.585 \AA . The five-coordinate orientation of the two His residues forms an almost square-pyramidal complex such that the N_1 of $[\text{CO},\text{N}_1]$ ligand is the apex of the pyramid (Figure 2). This complex is $6-28 \text{ kJ/mol}$ higher in 298 K free energy than the six-coordinate $[\text{CO},\text{N}_\alpha,\text{N}_1]/[\text{CO},\text{N}_\alpha,\text{N}_1]$ CS/CS structure. Several other CS/CS, CS/SB, and SB/SB combinations were attempted such that the zinc would be binding to either four, five, or six sites in the His ligands, but these are sufficiently high in energy ($\Delta\Delta G_{298\text{K}} \geq 17 \text{ kJ/mol}$) at all levels of theory (Table 2) that they are not expected to comprise greater than 1% of the reactant ions.

Similar low-energy structures were found for the $\text{Cd}^{2+}(\text{His})_2$ system (Table 2). Here the 298 K free energy GS at the DFT levels is again a CS/SB configuration, $[\text{CO},\text{N}_\alpha,\text{N}_1]\text{tgcc}/[\text{CO}_2^-]-\text{c}_{\text{N}1}\text{tgc}$; however, this complex is $4-6 \text{ kJ/mol}$ higher in 0 K enthalpy at the DFT levels and is disfavored in both 0 K enthalpy and 298 K free energy by $32-42 \text{ kJ/mol}$ at MP2(full). Instead

the 0 K GS at the DFT and MP2(full) levels is a CS/CS complex with C_2 symmetry, namely, the $[\text{CO},\text{N}_\alpha,\text{N}_1]\text{tgcc}/[\text{CO},\text{N}_\alpha,\text{N}_1]-\text{tgcc}$ conformer, which agrees with the overall 298 K GS predicted by MP2(full). Although there are similarities between the two $[\text{CO},\text{N}_\alpha,\text{N}_1]/[\text{CO},\text{N}_\alpha,\text{N}_1]$ structures of the Zn and Cd systems, the larger Cd ion has a small but noticeable effect on the coordination behavior as well as the resulting relative energetics. The larger size of the Cd^{2+} ion (ionic radius = 0.99 \AA^{41}) allows for an easier 6-fold coordination of the two histidines to the metal such that the two CO groups are coordinated closer to the metal with $\text{Cd}-\text{O}$ distances of 2.652 \AA . This distance is 0.312 \AA shorter than the $\text{Zn}-\text{O}$ bond in the analogous CS/CS structure discussed above for $\text{Zn}^{2+}(\text{His})_2$ but is still longer by 0.223 \AA compared to the $\text{Cd}-\text{O}$ distance of the carbonyl in the CS ligand of $[\text{CO},\text{N}_\alpha,\text{N}_1]\text{tgcc}/[\text{CO}_2^-]\text{c}_{\text{N}1}\text{tgc}$. The longer $\text{Cd}-\text{O}$ distances in the CS/CS complex again result from slight crowding around the cadmium ion, although this crowding has substantially decreased compared to the Zn system. Finally, compared to the predicted DFT GS of the $\text{Zn}^{2+}(\text{His})_2$ system, the analogous structure for $\text{Cd}^{2+}(\text{His})_2$ is $[\text{CO},\text{N}_\alpha,\text{N}_1]\text{tgcc}/[\text{CO}^-, \text{N}_\alpha]\text{c}_{\text{N}1}\text{cg}$ and is $7-9 \text{ kJ/mol}$ higher in 298 K free energy (40 kJ/mol at MP2(full)). Similar to $\text{Zn}^{2+}(\text{His})_2$, several other higher energy isomers were calculated using CS/CS, CS/SB, and SB/SB configurations (Table 2 and Supporting Information, Table S2); however, because these conformations are high in 298 K free energy, their spectra will not be compared to experimental spectra below and their structures will not be discussed explicitly here.

IRMPD Spectroscopy. Photodissociation spectra of $\text{CdCl}^+(\text{His})$, $[\text{Zn}(\text{His}-\text{H})]^+$, $[\text{Cd}(\text{His}-\text{H})]^+$, $\text{Zn}^{2+}(\text{His})_2$, and $\text{Cd}^{2+}(\text{His})_2$ were examined from ~ 550 to slightly past 1800 cm^{-1} (Figure 3). For $\text{CdCl}^+(\text{His})$, the photodissociation pathways correspond to loss of H_2O , NH_3 , OH , and $\text{OH} + \text{CO}$. The photo-dissociation of $[\text{M}(\text{His}-\text{H})]^+$ species mainly resulted in loss of CO_2 . For $\text{M}^{2+}(\text{His})_2$, photodissociation resulted in fragmentation and charge separation forming $[\text{M}(\text{His}-\text{H})]^+ + \text{H}^+(\text{His})$ products, with the $\text{H}^+(\text{His})$ product undergoing subsequent loss of H_2O and $\text{H}_2\text{O} + \text{CO}$. The IRMPD action spectra shown correspond to the relative intensity of all product ions as a function of laser wavelength. Spectra of individual product masses and parent ion depletion spectra were also generated for comparison and are similar to the overall corresponding yield spectrum for the monomeric and dimeric species.

Comparison of the IRMPD spectra in Figure 3 shows the similarities between the spectra of the Zn- and Cd-containing species. The experimental bands are identified on the basis of previous work^{14-16,19-21,39,40} as well as comparisons to theoretical spectra. From this, the lines drawn through all the spectra at ~ 610 , ~ 1155 , and $\sim 1725 \text{ cm}^{-1}$ mark the three major bands in the $\text{CdCl}^+(\text{His})$ spectra. The 610 cm^{-1} band is primarily a COH wagging motion, although there are contributions of an NH_2 rocking motion and imidazole wagging, as discussed below. The 1155 cm^{-1} band is primarily a COH bending motion of the free OH in a charge-solvated structure, although appreciable $\text{HN}_\alpha\text{CH}$ and HN_3CH bending motions are involved as well. Notably, the $[\text{M}(\text{His}-\text{H})]^+$ spectra do not exhibit the band at $\sim 1155 \text{ cm}^{-1}$, because the carboxylic acid terminus is now deprotonated. Instead a sharp band at $\sim 1120 \text{ cm}^{-1}$ appears and is assigned as a $\text{HN}_\alpha\text{CH}$ bend. Both bands at ~ 1155 and $\sim 1120 \text{ cm}^{-1}$ are observed in the $\text{Zn}^{2+}(\text{His})_2$ spectrum, whereas the $\text{Cd}^{2+}(\text{His})_2$ has the band at $\sim 1155 \text{ cm}^{-1}$ and a shoulder on the red side of this band at 1120 cm^{-1} . This strong band at 1155 cm^{-1} suggests the presence of at least one CS ligand in the dimer spectra,

whereas the band at 1120 cm^{-1} may demonstrate carboxylate character, suggesting a salt-bridge conformation. The band at 1725 cm^{-1} in the $\text{CdCl}^+(\text{His})$ spectrum is the $\text{C}=\text{O}$ stretch of

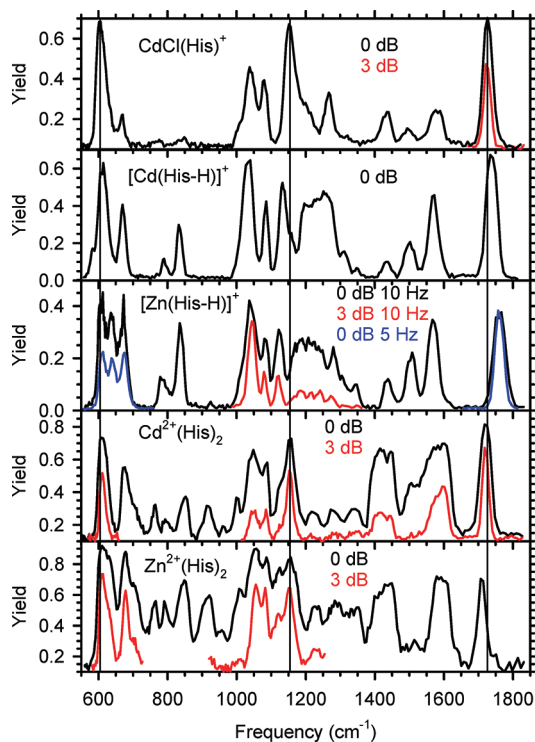


Figure 3. IRMPD spectra of $\text{CdCl}^+(\text{His})$, $[\text{Cd}(\text{His}-\text{H})]^+$, $[\text{Zn}(\text{His}-\text{H})]^+$, $\text{Zn}^{2+}(\text{His})_2$, and $\text{Cd}^{2+}(\text{His})_2$ complexes. Spectra taken with attenuated laser power (in decibels) or at reduced laser repetition rate are indicated in color. Solid lines at 610 , 1155 , and 1725 cm^{-1} are drawn to approximate the COH wagging, COH bending, and $\text{C}=\text{O}$ stretch of $\text{CdCl}^+(\text{His})$, respectively.

the carbonyl and shifts toward the blue for both the $[\text{M}-(\text{His}-\text{H})]^+$ spectra, red shifts for the $\text{Zn}^{2+}(\text{His})_2$ spectrum, and remains for the $\text{Cd}^{2+}(\text{His})_2$ spectrum. These shifts will be discussed in more detail along with the remaining bands in the spectra when compared to theory in the sections below.

Comparison to Theory: $\text{CdCl}^+(\text{His})$. Figure 4 shows the experimental IRMPD action spectrum along with calculated IR linear absorption spectra and relative 298 K free energies (at the B3LYP and MP2(full) levels) for the lowest-energy structures of $\text{CdCl}^+(\text{His})$. For the most part, the calculated IR spectra of complexes having the same metal binding sites are very similar such that a comparison with the lowest-energy conformer of each type of His coordination is sufficient for identification. The predicted spectra of the low- and high-energy complexes are compared to experimental spectra for all systems examined in this paper in the Supporting Information, Figure S3. It should be remembered that the experimental IRMPD intensities are not always reproduced by the calculated one-photon linear absorption spectrum, but the relative intensities between bands often offer a good qualitative comparison to experiment. As mentioned above, the most intense and distinctive bands are the carbonyl stretch at $\sim 1720\text{ cm}^{-1}$ and COH bending at $\sim 1155\text{ cm}^{-1}$. The positions and large intensities of both bands in the experimental spectrum suggest that there is a significant population of a CS structure.

The $[\text{CO}, \text{N}_\alpha, \text{N}_1]$ structure is by far the lowest in energy and, for an equilibrium distribution of complexes at 298 K, should comprise more than 99% of the reactant ions. The predicted $\text{C}=\text{O}$ band is located at 1720 cm^{-1} , in excellent agreement with experiment. For comparison, this band for $\text{Ca}^{2+}(\text{His})$ is located at $\sim 1680\text{ cm}^{-1}$. The blue shift of the $\text{C}=\text{O}$ band in the $\text{CdCl}^+(\text{His})$ system as compared to the similarly sized Ca^{2+} ion is likely a consequence of the Cl^- spectator ion, which induces longer M–O coordination to the CdCl^+ and therefore less perturbation of the $\text{C}=\text{O}$ stretch. The $\text{C}=\text{O}$ stretching band is by far the most diagnostic when comparing the spectra of the

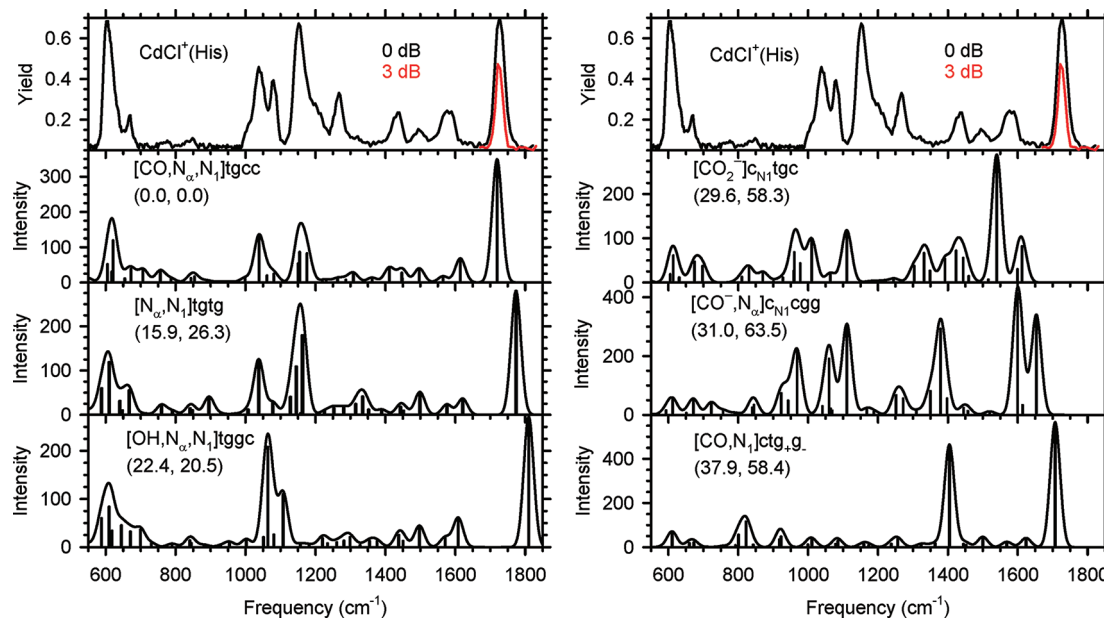


Figure 4. Comparison of the experimental IRMPD spectrum of $\text{CdCl}^+(\text{His})$ with IR spectra of six low-energy conformers predicted at the B3LYP/Def2TZVP level. A spectrum taken with attenuated laser power (in decibels) is indicated in color. Relative 298 K free energies from Table 1 are given in parentheses calculated at the B3LYP and MP2(full) levels using a Def2TZVPP basis set.

higher energy structures. This experimental band does not agree in position or shape to the predicted spectra of the higher energy SB complexes (Figure 4). The predicted CO_2^- asymmetric stretch (ν_{asym}) in the $[\text{CO}_2^-]_{\text{CN}_1\text{tgc}}$ SB complex is at 1549 cm^{-1} , much lower in frequency than the $\text{C}=\text{O}$ stretch of CS complexes, a shift seen previously¹⁵ between similarly coordinated complexes of His. The ν_{asym} of the CO_2^- is intrinsically lower in frequency than the $\text{C}=\text{O}$ stretch. The ν_{asym} of the coordinated CO^- in the $[\text{CO}^-, \text{N}_\alpha]$ complex is at $\sim 1600 \text{ cm}^{-1}$, higher in frequency than the ν_{asym} of the CO_2^- , also in agreement with previous calculations by Dunbar et al. on $\text{Ba}^{2+}(\text{His})$ and $\text{Ca}^{2+}(\text{His})$.¹⁵ Although there is no signature salt-bridge band predicted by theory, the $\text{CdCl}^+(\text{His})$ spectrum has little to no salt-bridge characteristics based on comparisons to the individual calculated spectra of the SB complexes. Therefore, it is unlikely that a SB complex is formed in the experiment.

The predicted $\text{C}=\text{O}$ stretches of the other CS complexes have shapes similar to experiment, but do not agree in position (although this could be an artifact of the scaling factor chosen here) (Figure 4). Although the $\text{C}=\text{O}$ stretch of the $[\text{CO}, \text{N}_1]$ complex agrees within 15 cm^{-1} , the remaining bands are in poor agreement with experiment. In the complexes where the metal is not coordinated to the carbonyl, $[\text{N}_\alpha, \text{N}_1]$ and $[\text{OH}, \text{N}_\alpha, \text{N}_1]$, the two $\text{C}=\text{O}$ stretches are both blue-shifted from experiment by 50 – 90 cm^{-1} . If we change the scaling factor applied to the predicted spectra such that this band agrees with experiment (requiring values of 0.927 – 0.945), then the lower frequency bands will be in poor agreement. Overall, the tridentate $[\text{CO}, \text{N}_\alpha, \text{N}_1]$ conformers provide the best agreement with experiment for the $\text{C}=\text{O}$ stretch.

As mentioned above, the band at 1155 cm^{-1} is indicative of a CS structure, because it involves the free OH motions of the carboxylic acid and therefore is not observed in any of the SB structures (Figure 4). This band is also shifted to lower frequencies in the $[\text{OH}, \text{N}_\alpha, \text{N}_1]$ complex. In the GS complex, the intense band at $\sim 1155 \text{ cm}^{-1}$ is primarily a result of the COH bending mode with contributions of $\text{HN}_\alpha\text{CH}$ and HN_3CH bending motions. There are additional intense bands in the spectrum that are identified as the NH_2 wagging at $\sim 1040 \text{ cm}^{-1}$ and COH wagging at $\sim 610 \text{ cm}^{-1}$, but there are also contributions from wagging of the imidazole ring and a rocking motion of the NH_2 group. A sideband of this main peak is centered at $\sim 670 \text{ cm}^{-1}$ and corresponds to a similar mode, namely, the HNC wagging of the N_3 in the imidazole side chain. Both bands predicted for the $[\text{CO}, \text{N}_\alpha, \text{N}_1]$ GS conformer agree nicely with experiment in both position and relative intensity. The experimental band at $\sim 1585 \text{ cm}^{-1}$ is believed to be the NH_2 bending motion and the predicted peak of the GS is shifted to higher frequencies by $\sim 25 \text{ cm}^{-1}$ from experiment. This deviation has been observed previously^{40,42–45} and is believed to be a consequence of strong anharmonic effects. The remaining bands in the range 1250 – 1500 cm^{-1} are different movements along the backbone and side chain of the amino acid. Overall, the large bands at $\sim 1725, 1155, 1040, 670$, and 610 cm^{-1} are each in excellent agreement with the predicted vibrations of the $[\text{CO}, \text{N}_\alpha, \text{N}_1]$ complex in positions and band shapes. This overall agreement suggests that this complex is predominately formed in the experiment and that the vibrational scaling factor applied here is accurate.

There are two peaks in the experimental spectrum that are not reproduced with high fidelity in the predicted spectrum of the $[\text{CO}, \text{N}_\alpha, \text{N}_1]$ GS at ~ 1080 and 1270 cm^{-1} . The first may be an imidazole ring in-plane CH bending mode, as assigned on the

basis of condensed-phase IR spectra of imidazole and histidine.^{46,47} A small contribution from these modes is observed in the predicted spectrum, but the experimental peak is more intense than predicted by theory in any of the calculated spectra (Figure 4). This phenomenon has also been reported previously by Prell and co-workers for the $\text{H}^+(\text{HisArg})$ system, who found a similar sharp band at 1080 cm^{-1} that was not reproduced by theory.²⁰ Assignment of this band as the neutral imidazole was confirmed by the addition of a second proton to form $\text{H}_2^{2+}(\text{HisArg})$, where the band in question decreases substantially as the imidazole is believed to be protonated, thereby altering its frequencies. The second unassigned band at 1270 cm^{-1} could be the ring stretch of the imidazole.⁴⁷ Given the large number of bands from 500 to 1500 cm^{-1} in the condensed-phase spectra of imidazole⁴⁷ and histidine,⁴⁶ as well as inconsistent matching to the IRMPD spectra, exact assignment of this as well as the other minor bands in the region measured for the experimental spectra is difficult. The lack of these two bands in the theoretical spectra is not surprising given that predicted vibrational frequencies are calculated using the harmonic oscillator approximation. As observed above, this multiple-photon experimental spectrum can lead to substantial shifts in bands with strong anharmonic tendencies such that these experimental bands could be shifted or the result of an overtone not calculated in the theoretical linear absorption spectrum. Likewise, the predicted intensity of strongly anharmonic modes can deviate substantially from experiment.

$[\text{M}(\text{His}-\text{H})]^+$. Comparing the experimental spectrum of $[\text{Cd}(\text{His}-\text{H})]^+$ to the predicted spectra of the low-energy structures, there is good agreement with that of the $[\text{CO}^-, \text{N}_\alpha, \text{N}_1]\text{-H}_{\text{COggc}}$ GS (Figure 5a). Here the major and minor bands discussed above are predicted well in peak position, and relative intensities are reasonable as well. This structure of the $[\text{CO}^-, \text{N}_\alpha, \text{N}_1]\text{-H}_{\text{COggc}}$ GS is similar to that determined to be the GS for the $\text{CdCl}(\text{His})^+$ complex, except the carboxylic acid is deprotonated and there is no spectator Cl^- ion. This allows the metal to be closer in distance to each coordination site, which will most likely be reflected in the position of certain diagnostic bands like the $\text{C}=\text{O}$ stretch, as discussed in detail below.

The peak intensities of all the bands below 1600 cm^{-1} are smaller relative to the band at 1740 cm^{-1} in the predicted GS spectrum, whereas they appear much more intense in experiment. This is because the experimental spectra presented in this paper have not been corrected for the gradual decrease of laser power toward the blue edge of the spectra (up to 20 mJ per macropulse in this region). An example of a power corrected spectrum for $[\text{Cd}(\text{His}-\text{H})]^+$ is given in the Supporting Information, Figure S4. Once power-corrected, the intensity of the $\text{C}=\text{O}$ stretch increases (by a factor of about 2.2) and the intensity of the lower frequency bands relative to the $\text{C}=\text{O}$ stretch agrees well with that predicted in the GS spectrum. We have chosen not to power-correct experimental spectra for this paper because shapes and positions of the minor lower frequency bands are then more easily examined.

The $[\text{Cd}(\text{His}-\text{H})]^+$ spectrum is similar to that of the $\text{CdCl}^+(\text{His})$ complex over the wavelength range examined here (Figure 3). One subtle difference with respect to the two spectra is in the increased intensity of the minor bands in the deprotonated complex. Specifically, the experimental band at 610 cm^{-1} decreases relative to the band at 670 cm^{-1} , because there is no COH wagging contribution in the deprotonated complex. This peak is predicted at 614 cm^{-1} for the $[\text{CO}^-, \text{N}_\alpha, \text{N}_1]\text{-H}_{\text{COggc}}$ GS and comprises the wagging of the imidazole side chain along with

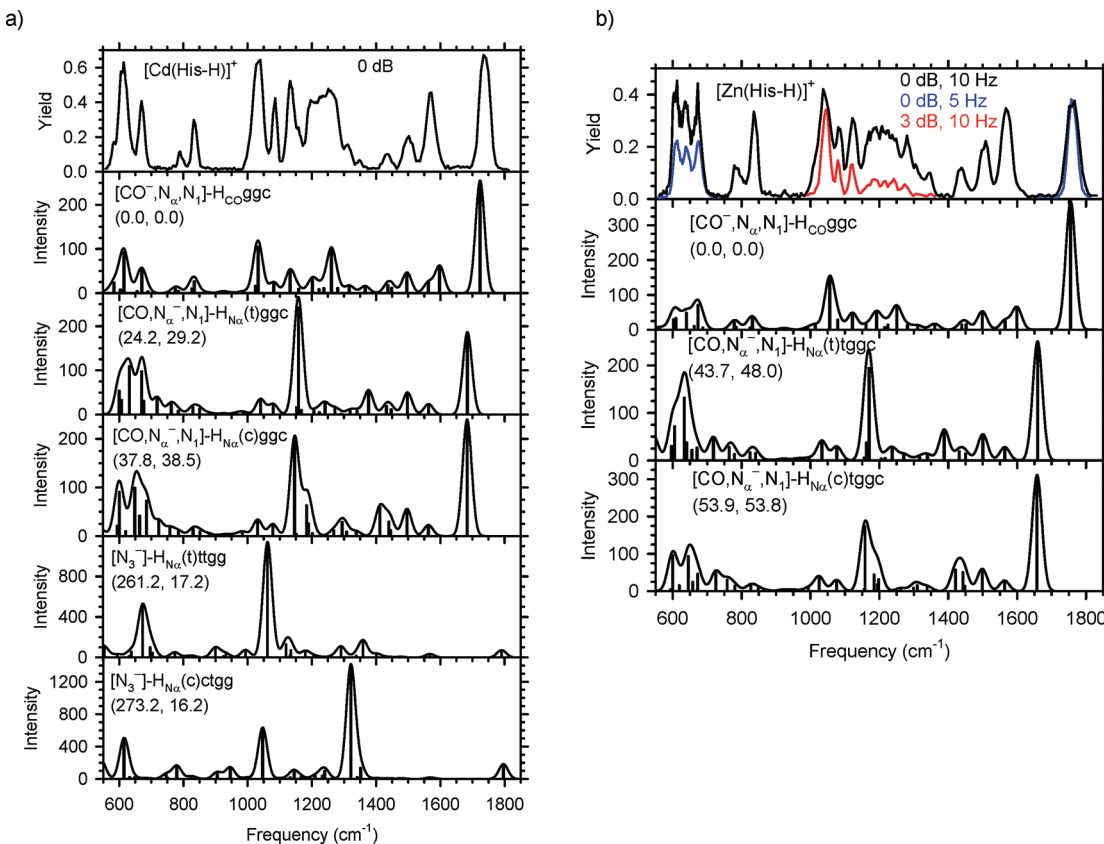


Figure 5. Comparison of the experimental IRMPD spectra of $[Cd(\text{His}-\text{H})]^+$ and $[Zn(\text{His}-\text{H})]^+$ with IR spectra of selected low-energy conformers predicted at the B3LYP/Def2TZVP and B3LYP/6-311+G(d,p) levels. Spectra taken with attenuated laser power (in decibels) or at reduced laser repetition rate are indicated in color. Relative 298 K free energies from Table 1 are given in parentheses calculated at the B3LYP and MP2(full) levels.

the NH_2 rocking motion, which were minor contributions to this band discussed above. The peak at 670 cm^{-1} corresponds to the HNC wag of N_3^- in the side chain in both species. Also, two bands at 790 and 835 cm^{-1} appear, which were only hinted at in the $\text{CdCl}^+(\text{His})$ spectrum. These two bands are C–C stretches and CH_2 rocking motions along the backbone causing the coordinated oxygen and α -amino groups to stretch closer to the metal ion. The shapes, positions, and relative intensity of these two bands are only reproduced in the tridentate complex when the deprotonation occurs on the carboxylic acid terminus, forming the $[\text{CO}^-, \text{N}_\alpha, \text{N}_1]\text{-HCOggc}$ GS (Figure 5a). Deprotonation at N_α broadens these bands considerably, and relative intensities are poorly reproduced. The $[\text{Cd}(\text{His}-\text{H})]^+$ spectrum also has a sharp band at 1130 cm^{-1} and a broad band from 1200 to 1275 cm^{-1} . The band at $\sim 1130 \text{ cm}^{-1}$ is the $\text{HN}_\alpha\text{CH}$ bend, which is red-shifted by $\sim 25 \text{ cm}^{-1}$ from the peak in the $\text{CdCl}^+(\text{His})$ spectrum, where it was attributed primarily to the COH bend, along with contributions from the $\text{HN}_\alpha\text{CH}$ bend, as discussed above. The decrease in intensity and 25 cm^{-1} red shift in band position can be expected from the absence of the COH bend and a long-range attractive interaction between the proton on the α -amino group and the oxygens of the carboxylate. Interestingly, there is a small mode observable in the predicted spectra at $\sim 1155 \text{ cm}^{-1}$, assigned to the HN_3^-CH bending motion. This motion is also present though unresolved from the COH wag in the $\text{CdCl}^+(\text{His})$ spectrum, but it is unaffected by the CO_2^- moiety formed by deprotonation. The broad band from 1200 to 1275 cm^{-1} includes the symmetric stretch (ν_{sym}) of CO_2^- at

1260 cm^{-1} , as well as other bends and twists along the backbone and side chain. This assignment agrees with previous vibrations assigned¹⁴ to the Phe–H ligand in the $[\text{Zn}(\text{Phe})(\text{Phe}-\text{H})]^+$ complex. The small peaks at ~ 1300 and 1350 cm^{-1} are predicted in the theoretical spectrum of $[\text{CO}^-, \text{N}_\alpha, \text{N}_1]\text{-HCOggc}$ to be stretches of the ring and CH movements, also in agreement with the Phe–H assignments. The three bands from 1400 to 1600 cm^{-1} are also in relatively good agreement with the predicted spectrum, especially if the NH_2 umbrella motion at 1600 cm^{-1} is red-shifted somewhat experimentally because of the anharmonic effects noted above.

The most surprising difference between the $[\text{Cd}(\text{His}-\text{H})]^+$ and $\text{CdCl}^+(\text{His})$ spectra is that the ν_{asym} of the CO_2^- blue-shifted by $\sim 20 \text{ cm}^{-1}$ from the C=O stretch in the $\text{CdCl}^+(\text{His})$ spectrum. One might expect a red shift of this stretching band in the $[\text{Cd}(\text{His}-\text{H})]^+$ spectrum because of the carboxylate character in addition to the fact that the CO^- is coordinated 0.371 Å closer to the Cd^{2+} compared to the distance of the CO to CdCl^+ . In the $[\text{CO}^-, \text{N}_\alpha, \text{N}_1]\text{-HCOggc}$ GS, this molecular motion consists primarily of the stretch of the uncoordinated oxygen of the carboxylate group, whereas in the $\text{CdCl}^+(\text{His})$ complex, this band corresponds to the coordinated oxygen of the carbonyl. This band position and movement of the CO_2^- is in agreement with the behavior observed in the $[\text{Zn}(\text{Phe})(\text{Phe}-\text{H})]^+$ system (experimental $\text{CO}_2^- \nu_{\text{asym}} = 1736 \text{ cm}^{-1}$)¹⁴ and also agrees with the predicted spectrum of the calculated GS (Figure 5a).

Looking at the two predicted spectra of higher-energy tridentate complexes where the α -amino group is deprotonated

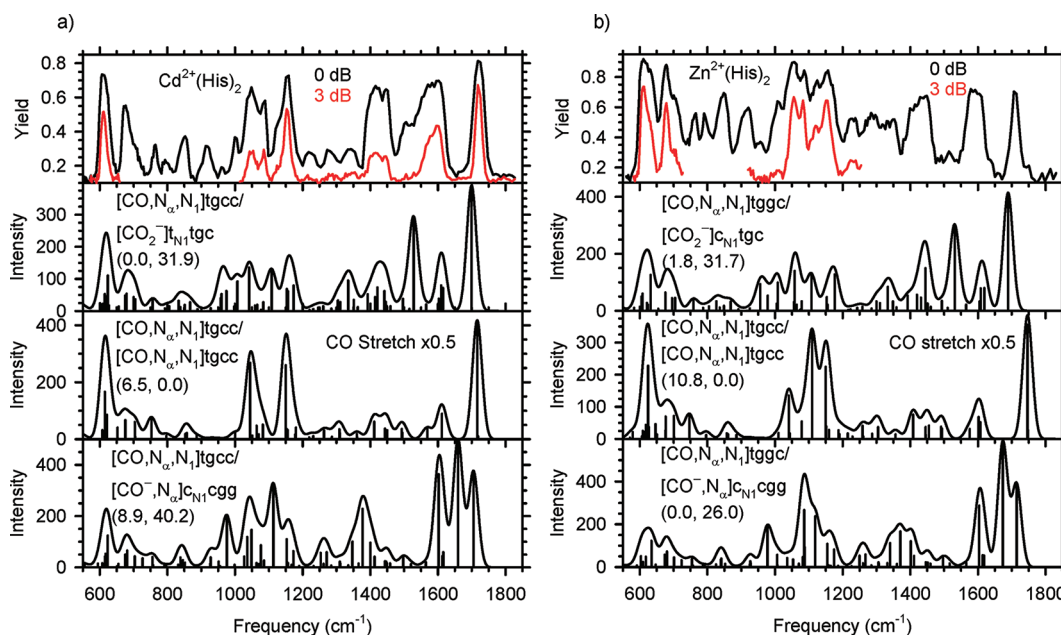


Figure 6. Comparison of the experimental IRMPD spectra of $\text{Cd}^{2+}(\text{His})_2$ and $\text{Zn}^{2+}(\text{His})_2$ with IR spectra of selected low-energy conformers predicted at the B3LYP/Def2TZVP and B3LYP/6-311+G(d,p) levels. Relative 298 K free energies from Table 2 are given in parentheses calculated at the B3LYP and MP2(full) levels. Spectra taken with attenuated laser power (in decibels) are indicated in color. The predicted $\text{C}=\text{O}$ stretch is scaled by 0.5 for the $[\text{CO},\text{N}_\alpha,\text{N}_1]/[\text{CO},\text{N}_\alpha,\text{N}_1]$ conformer of $\text{Cd}^{2+}(\text{His})_2$ and $\text{Zn}^{2+}(\text{His})_2$.

(Figure 5a), the main $\text{C}=\text{O}$ stretch feature consists of the movement of the metal-coordinated carbonyl group such that it is red-shifted from experiment by $\sim 55 \text{ cm}^{-1}$. The other bands of these predicted spectra are also in poor agreement with experiment in band position and relative intensity. Thus, these conformations do not appear to be formed experimentally, agreeing with the calculated relative energetics (Table 1). Figure 5a also shows the $[\text{N}_3]$ complexes, which are only 16–17 kJ/mol higher in 298 K free energy than the GS at the MP2(full) level. Comparing these spectra to experiment there is an immediate and obvious disagreement from the lack of a major $\text{C}=\text{O}$ stretch. Instead, the predominant bands in the predicted spectra result from wagging motions of the COH at $\sim 1320 \text{ cm}^{-1}$ and CN_αH at $\sim 1055 \text{ cm}^{-1}$. The major differences between the two linear absorption spectra of the $[\text{N}_3]$ complexes come from the differences in the hydrogen-bonding network and orientation of the α -amino group described in the section above.

The $[\text{Zn}(\text{His}-\text{H})]^+$ spectrum is very similar to its Cd counterpart (Figure 3). As for $[\text{Cd}(\text{His}-\text{H})]^+$, the $\text{Zn}[\text{CO}^-, \text{N}_\alpha, \text{N}_1]-\text{H}_{\text{COggc}}$ GS is in excellent agreement with the experimental spectrum (Figure 5b). The ν_{asym} of the CO_2^- agrees in both position and shape to the GS. Different from the Cd system, the $[\text{Zn}(\text{His}-\text{H})]^+$ spectrum has three low-frequency bands at ~ 605 , 640 , and 670 cm^{-1} . The positions of these bands agree within 5 cm^{-1} with three similarly shaped bands in the theoretically predicted spectrum of $[\text{CO}^-, \text{N}_\alpha, \text{N}_1]-\text{H}_{\text{COggc}}$. Specifically, the predicted band at 610 cm^{-1} consists of the wagging and bending of the imidazole side chain, the frequency at 642 cm^{-1} is the $\text{N}_\alpha\text{H}_2$ rock, and the peak at 673 cm^{-1} is the HN_3C wag. Differences in the splitting of these bands compared to the Cd system are most likely because of the tighter coordination of the Zn ion to His-H, as reflected in the smaller coordination distances. The remainder of the bands are similar to those discussed above for $[\text{Cd}(\text{His}-\text{H})]^+$, and similar to the Cd system, the high

energy isomers of $[\text{Zn}(\text{His}-\text{H})]^+$ do not agree with experiment (Figure 5b and Supporting Information, Figure S2). As a whole, the experimental spectra of the monomeric species agree very well with the spectra of the calculated GS conformers, which are overwhelmingly favored by the relative energetics at all three levels of theory for all three systems.

$\text{Cd}^{2+}(\text{His})_2$. Up until this point the spectral comparisons and relative energetics of the monomeric species consistently demonstrate a preference for the tridentate binding of a charge-solvated His and a tridentate His-H (with a deprotonated carboxylic acid terminus) to Cd and Zn. Comparing the experimental spectrum of $\text{Cd}^{2+}(\text{His})_2$ to the $\text{CdCl}^+(\text{His})$ spectrum, the position of the $\text{C}=\text{O}$ stretch is fairly similar at $\sim 1720 \text{ cm}^{-1}$ (Figure 3), most likely a consequence of at least one similarly coordinated charge-solvated ligand. The similar position of the $\text{C}=\text{O}$ stretch compared to the $\text{CdCl}^+(\text{His})$ complex also suggests that the coordination to the CS carbonyl is relatively long in the dimer complex, probably because of the increased crowding around the metal, as discussed above. The $\text{Cd}^{2+}(\text{His})_2$ spectrum also has a large peak at $\sim 1150 \text{ cm}^{-1}$, indicative of the carboxylic acid free OH motion, which is also consistent with CS character. However, as mentioned above, the dimeric spectrum has broadening on the red side of this peak at $\sim 1120 \text{ cm}^{-1}$ (much smaller intensity relative to the peak at 1150 cm^{-1} in the 3 dB spectrum). There is no such broadening in the $\text{CdCl}^+(\text{His})$ experimental spectrum, but there are bands at $\sim 1110 \text{ cm}^{-1}$ in the predicted spectra of the SB structures calculated for this reactant, namely, the complexes containing the $[\text{CO}_2^-]$ and $[\text{CO}^-, \text{N}_\alpha]$ ligands (Figure 6). The position of this broadening at 1120 cm^{-1} is similar to the $\text{HN}_\alpha\text{CH}$ bending mode discussed above for the $[\text{Cd}(\text{His}-\text{H})]^+$ spectrum, a spectrum with carboxylate characteristics. In comparison to the CS $\text{CdCl}^+(\text{His})$ spectrum, the peaks from 1400 to 1600 cm^{-1} in the $\text{Cd}^{2+}(\text{His})_2$ spectrum are much broader and have grown in intensity relative to the $\text{C}=\text{O}$

stretch, which is suggestive of contributions from SB conformers. In addition, there are bands in the $1200\text{--}1400\text{ cm}^{-1}$ range, also similar to the $[\text{Cd}(\text{His}-\text{H})]^+$ spectrum. There are new bands at 760 , 925 , 965 , and 1005 cm^{-1} , which were not observed in the CS spectrum of $\text{CdCl}^+(\text{His})$ (Figure 4) or the spectrum of $[\text{Cd}(\text{His}-\text{H})]^+$ (Figure 5). Finally, the shapes and positions of the bands in the $\text{Cd}^{2+}(\text{His})_2$ spectrum are similar to those reported in the IRMPD spectrum of $\text{Cd}^{2+}(\text{Trp})_2$, which was assigned as a CS/SB conformation by Dunbar et al.¹⁹ These authors observed similar, subtle changes between the monomer and dimer spectra of Trp complexed with Cd and assigned a CS and CS/SB configuration to these two spectra, respectively. On the basis of these observed changes in the experimental spectrum of the dimeric species and comparisons to the reported spectra in the literature, one of the His ligands is in a CS formation while the other is possibly SB, but contributions from CS/CS structures cannot be rejected yet.

The $\text{C}=\text{O}$ stretch of the predicted spectrum of the C_2 symmetric $[\text{CO}_2\text{N}_\alpha\text{N}_1]\text{tgcc}/[\text{CO}_2\text{N}_\alpha\text{N}_1]\text{tgcc}$ complex agrees best with experiment in both band position and shape (Figure 6a). The remaining predicted bands are also in relatively good agreement in peak position, although the intense contribution of the $\text{C}=\text{O}$ stretching band obscures the smaller peaks. Obviously, there is poor agreement in the relative intensities between the $\text{C}=\text{O}$ stretch and the lower frequency bands, in part because the gradually changing laser power is not accounted for or possibly by contributions of a SB conformer as discussed below. Therefore, we have scaled the $\text{C}=\text{O}$ stretching band in the CS/CS predicted spectrum by a factor of 0.5 to better simulate the experimental spectrum (uncorrected for laser power) and to more clearly see the lower frequency bands. This allows for the clear identification of the band at 760 cm^{-1} , which is a OCOH bend, and is present in all CS/CS or CS/SB spectra. Because of the complexity of this dimer system, there is a large number of bands and there is no single mode diagnostic of a SB ligand. However, as suggested by the comparisons of experimental spectra above, there are no bands in the CS/CS spectrum at ~ 925 or 960 cm^{-1} , and the large broad experimental bands in the range of $1200\text{--}1650\text{ cm}^{-1}$ are not reproduced with high fidelity. However, comparison of the 0 and 3 dB spectra shows that the $\text{C}=\text{O}$ stretching band is easily saturated, such that the relative intensities between this band and those from 1200 to 1650 cm^{-1} in the 3 dB spectrum agree well with predicted relative intensities of the CS/CS MP2(full) GS. In addition, this CS/CS conformer has no predicted vibrational modes at 1120 cm^{-1} , a mode that may be indicative of some carboxylate characteristics, as discussed for the $[\text{Cd}(\text{His}-\text{H})]^+$ spectrum. The $[\text{CO}_2\text{N}_\alpha\text{N}_1]\text{tgcc}/[\text{CO}_2\text{N}_\alpha\text{N}_1]\text{-tgcc}$ complex is the MP2(full) GS, but it is $4.4\text{--}6.5\text{ kJ/mol}$ higher in 298 K free energy at the DFT levels (Table 2).

The DFT GS is a CS/SB complex, $[\text{CO}_2\text{N}_\alpha\text{N}_1]/[\text{CO}_2^-]$, which is higher in MP2(full) 298 K free energy by 32 kJ/mol . Comparing the predicted spectrum of this CS/SB complex to experiment, the $\text{C}=\text{O}$ stretching band of the CS ligand is red-shifted from experiment by $\sim 20\text{ cm}^{-1}$, peaking at 1700 cm^{-1} . The ν_{asym} stretch of the coordinated CO_2^- group peaks at 1527 cm^{-1} , in good agreement with the experimental shoulder $\sim 1520\text{ cm}^{-1}$, although the predicted intensity of this stretch is much higher than what is found experimentally. Additionally, there are predicted bands that involve the motion of the proton involved in the salt-bridge between the N_1 and N_α groups from ~ 920 to 1010 cm^{-1} and at 1110 cm^{-1} . These bands reproduce the position of those found in the experiment within

$3\text{--}20\text{ cm}^{-1}$, although again the relative intensities are not well predicted.

The remaining bands from 1200 to 1600 cm^{-1} are difficult to assign, as both predicted GS spectra have vibrational modes here. However, these bands in the CS/CS spectrum are very low in intensity relative to the predicted COH wagging, NH_2 wagging, COH bending, and $\text{C}=\text{O}$ stretching peaks at 610 , 1045 , 1150 , and 1716 cm^{-1} , respectively. More intense broad bands are found in the DFT GS CS/SB spectrum, similar to experiment (Figure 6a), suggesting possible contributions of this conformer to the experimental spectrum. The positioning of these bands is slightly off from experiment, which could be a result of large anharmonic affects in this region, as discussed above. The lower frequency bands at ~ 610 and 675 cm^{-1} are reproduced with either predicted spectrum, although the relative intensity between these two bands is predicted slightly better using the CS/SB conformer. This is because the band at 610 cm^{-1} decreases in intensity from the lack of the COH wagging motion in the SB ligand (as seen in the $[\text{Cd}(\text{His}-\text{H})]^+$ spectrum) and the HNC band at 675 cm^{-1} grows in intensity because of the additional wagging movements of the protonated N_1 and N_3 in the side chain. The predicted spectrum of the $[\text{CO}_2\text{N}_\alpha\text{N}_1]\text{tgcc}/[\text{CO}_2^-\text{N}_\alpha]\text{c}_1\text{cg}$ complex is also given in Figure 6a, but the three intense and sharp bands at ~ 1600 (proton movement between the N_1 and CO_2^- and NH_2 bands), 1660 (ν_{asym} of the coordinated oxygen in the CO_2^-), and 1705 cm^{-1} ($\text{C}=\text{O}$ stretch) do not agree well with experiment.

Overall it appears that the experimental spectrum has bands unique to at least one CS ligand, but it also has bands indicative of a ligand with a SB structure, which can be described by the predicted spectrum of the $[\text{CO}_2\text{N}_\alpha\text{N}_1]/[\text{CO}_2^-]$ DFT GS. The latter assignment is in agreement with that made by Dunbar et al.¹⁹ for $\text{Cd}^{2+}(\text{Trp})_2$; however, the main $\text{C}=\text{O}$ stretching band is best described by the $[\text{CO}_2\text{N}_\alpha\text{N}_1]/[\text{CO}_2\text{N}_\alpha\text{N}_1]$ MP2(full) GS, which also predicts most of the other bands reasonably well. Given that the levels of theory disagree as to which complex is the GS and DFT predicts relatively close energetics between these two structures, it is difficult to make an unambiguous assignment of one particular complex to the $\text{Cd}^{2+}(\text{His})_2$ spectrum. A combination of the CS/CS and CS/SB structures probably would reproduce the observed spectrum the best.

Zn²⁺(His)₂. Comparing the $\text{Cd}^{2+}(\text{His})_2$ spectrum to that of $\text{Zn}^{2+}(\text{His})_2$ there are obvious similarities with slight differences in the spectral signatures (Figure 3). Notably, the $\text{C}=\text{O}$ stretching band has shifted from $\sim 1720\text{ cm}^{-1}$ in the Cd^{2+} spectrum to $\sim 1710\text{ cm}^{-1}$ in the Zn^{2+} spectrum, implying a closer coordination of the carbonyl in the CS ligand to the Zn^{2+} . The width of this peak also decreases slightly from 23 to 17 cm^{-1} , but this could be a consequence of saturation, which unfortunately was not collected at 3 dB attenuation. The experimental bands from 920 to 1010 and $\sim 1120\text{ cm}^{-1}$ are assigned above to the proton participating in the SB of the $[\text{CO}_2^-]$ complex. These bands are present in the spectrum and have also grown in intensity compared to the same peaks in the $\text{Cd}^{2+}(\text{His})_2$ spectrum, although again this could be a consequence of saturation of the $\text{C}=\text{O}$ stretch. The band at 1120 cm^{-1} is more clearly observed, compared to the low-frequency shoulder on the COH bending band observed for $\text{Cd}^{2+}(\text{His})_2$. However, there appears to be less saturation of the major bands at 610 , 1050 , 1075 , 1110 , and 1150 cm^{-1} in the $\text{Zn}^{2+}(\text{His})_2$ system; i.e., the decrease in intensity between the 0 and 3 dB spectra is not as drastic as for $\text{Cd}^{2+}(\text{His})_2$. Saturation may be more easily obtained with the

CS/CS complex because there are two coordinating carbonyls. The COH bend remains at 1150 cm^{-1} , implying the presence of at least one His ligand with a CS structure. These observations suggest a similar structure or combination of structures being present in the $\text{Zn}^{2+}(\text{His})_2$ complex as for $\text{Cd}^{2+}(\text{His})_2$. This indicates that there are only small structural changes to the experimental reactant when Cd is substituted for Zn in the gas phase, in agreement with our assignments of similar structures to the monomeric species.

Looking at the predicted spectrum of the C_2 symmetric $[\text{CO},\text{N}_\alpha,\text{N}_1]\text{tgcc}/[\text{CO},\text{N}_\alpha,\text{N}_1]\text{tgcc}$ complex, the predicted $\text{C}=\text{O}$ stretch is located at 1747 cm^{-1} , a blue shift of $\sim 37\text{ cm}^{-1}$ from the experimental peak at $\sim 1710\text{ cm}^{-1}$ (Figure 6b). Such a blue shift is induced by the longer CO coordination to the metal, a result of the steric hindrance of these His ligands around the smaller zinc dication, as discussed above. Instead, there is a small feature in the experimental spectrum near 1750 cm^{-1} , which may be a small contribution from this blue-shifted $\text{C}=\text{O}$ stretch of the CS/CS complex. The less chelated structures, including ones containing a SB His ligand, are favored by the relative DFT energetics.

However, the evidence for a CS/SB conformer is hardly conclusive based on spectral comparisons to theory. The predicted $\text{C}=\text{O}$ stretch of the carbonyl in the CS ligand of the $[\text{CO},\text{N}_\alpha,\text{N}_1]\text{tgcc}/[\text{CO}_2^-]$ complex is again red-shifted from the experimental spectrum by $\sim 20\text{ cm}^{-1}$, similar to what was found for the corresponding structure of $\text{Cd}^{2+}(\text{His})_2$. Additionally, this complex is no longer the DFT GS, instead the $[\text{CO},\text{N}_\alpha,\text{N}_1]\text{tgcc}/[\text{CO}^-, \text{N}_\alpha]$ is 2–3 kJ/mol lower in 298 K free energy at the B3LYP and B3P86 levels. The predicted spectrum of this GS is again in relatively poor agreement with experiment. The large ν_{asym} of the CO_2^- at $\sim 1673\text{ cm}^{-1}$ is split with the $\text{C}=\text{O}$ stretch of the CS ligand at $\sim 1714\text{ cm}^{-1}$ and has no match in the experimental spectrum. To try to achieve better spectral comparisons for this system, optimization and frequency calculations were performed on these $\text{Zn}^{2+}(\text{His})_2$ complexes at the B3LYP/Def2-TZVP level anticipating that the size consistent basis set may better describe this system. However, the resulting structures and vibrations were similar to those using the 6-311+G(d,p) basis set. Finally, CS/CS and CS/SB structures were rebuilt to try and change distances from the coordination sites to the metal, to better fit the band positions of the $\text{C}=\text{O}$ and CO_2^- ν_{asym} stretches in the experimental spectrum, but during the optimization steps these structures returned to the low-energy structures already presented here. Less chelated CS/CS, CS/SB, and SB/SB conformers were calculated and the spectra of higher-energy structures were compared to experiment; however, none offer better agreement to the IRMPD spectrum (Supporting Information, Figure S5). Perhaps a more extensive conformational search is required.

From these comparisons to the predicted spectra and from the ambiguous relative energetics, it seems that conventional theoretical calculations struggle with predicting structural parameters and vibrational modes in this complicated two-ligand system featuring a small highly charged metal. Given that the experimental spectrum of $\text{Zn}^{2+}(\text{His})_2$ is similar to the $\text{Cd}^{2+}(\text{His})_2$ spectrum, it seems that similar structural assignments of the $\text{Zn}^{2+}(\text{His})_2$ complex can be made based on the spectral comparisons outlined for the $\text{Cd}^{2+}(\text{His})_2$. Dunbar et al.¹⁹ assigned a CS/SB structure as the GS for both the $\text{Zn}^{2+}(\text{Trp})_2$ and $\text{Cd}^{2+}(\text{Trp})_2$ spectra, where the CS/SB coordination is somewhat similar to the $[\text{CO},\text{N}_\alpha,\text{N}_1]/[\text{CO}_2^-]$ complex discussed above. Each metal

is coordinated similarly, although in the Trp system the metal is coordinated to the aromatic ring instead of the N_1 of the imidazole ring as in the His system. Our comparisons as well as the MP2(full) energetics suggest that the CS/CS $[\text{CO},\text{N}_\alpha,\text{N}_1]/[\text{CO},\text{N}_\alpha,\text{N}_1]$ structure may be a major contributor as well.

CONCLUSIONS

The role of the metal in the conformational dependence of histidine was investigated by measuring the IRMPD action spectra of monomeric histidine, deprotonated histidine, and dimeric histidine in the region of 550 – 1800 cm^{-1} for complexes with CdCl^+ , Cd^{2+} , and Zn^{2+} . Comparison of these experimental spectra with IR spectra calculated at the B3LYP/6-311+G(d,p) and B3LYP/Def2TZVP levels of theory identified the conformations likely present in the experiment. The monomeric species are unambiguously assigned as tridentate complexes of histidine to the metal. Specifically, for the $\text{CdCl}^+(\text{His})$ system, the amino acid forms a charge-solvated configuration coordinated to the carbonyl, N_1 of the imidazole side chain, and to the α -amino group in a $[\text{CO},\text{N}_\alpha,\text{N}_1]\text{tgcc}$ fashion. This assignment is clear from the strong $\text{C}=\text{O}$ stretch at $\sim 1720\text{ cm}^{-1}$ and the obvious presence of the free OH motion of the COH bend at $\sim 1150\text{ cm}^{-1}$. Through comparisons to the other monomeric spectra and to theory, it is found that the Cl^- spectator ion has little effect on the experimental spectrum with the possible exception of the position of the $\text{C}=\text{O}$ stretching band resulting from the longer coordination to the CO and lower overall charge transfer. The $[\text{M}(\text{His}-\text{H})]^+$ spectra are very similar for both Cd^{2+} and Zn^{2+} , and the structures identified as the primary component of both spectra had a deprotonated carboxylic acid terminus resulting in a $[\text{CO}^-, \text{N}_\alpha,\text{N}_1]$ configuration. Minor differences in the splitting and position of certain bands between the spectra of $[\text{Zn}(\text{His}-\text{H})]^+$ and $[\text{Cd}(\text{His}-\text{H})]^+$ are observed. Structural differences of these two complexes are also minor, and the small differences in the experimental spectra were most likely the result of the tighter coordination of the smaller Zn^{2+} metal. These spectral assignments agree with the assigned ground states calculated by all three levels of theory.

In contrast, the dimeric spectra of $\text{Cd}^{2+}(\text{His})_2$ and $\text{Zn}^{2+}(\text{His})_2$ were less conclusive partly because of the large size and complexity of these systems. Both experimental spectra have a large number of bands, making it difficult to definitively assign one configuration versus another. In addition, the calculated relative energetics disagree on the most stable configuration. The DFT levels favor a CS/SB binding of the two histidines, whereas MP2(full) strongly favors a CS/CS symmetric complex. The presence of at least one CS ligand is clear, as both spectra have strong bands resulting from the COH bend and $\text{C}=\text{O}$ stretch typical of a CS configuration. The $\text{Cd}^{2+}(\text{His})_2$ spectrum agrees fairly well with a six-coordinate CS/CS complex, although there are bands not accounted for in the predicted spectrum as well as discrepancies in the relative intensities. Comparisons to theoretically predicted spectra show that the identification of a SB ligand in the presence of a CS ligand is not straightforward. In the experimental spectra, there are small peaks from 900 to 1010 cm^{-1} , the growth of a peak at 1120 cm^{-1} , and broad bands in the 1350 – 1600 cm^{-1} range, which all suggest the presence of a SB ligand. The exact identification of the CS/SB configuration rests heavily on the detailed matching of the predicted spectra to experiment in regions that were shown to have strong anharmonic tendencies. Future IRMPD studies on these metals with

imidazole are probably warranted to make unambiguous assignments of these bands, given that theory is clearly not adequately describing some of these frequencies using simple harmonic oscillator methods.

Even without precise structural assignment of the $Zn^{2+}(His)_2$ and $Cd^{2+}(His)_2$, it seems that the spectra of both are quite similar to one another, in agreement with comparisons between the $[Zn(His-H)]^+$ and $[Cd(His-H)]^+$ spectra. Perhaps histidine is not susceptible to severe structural changes when replacing zinc with cadmium, as found for carbonic anhydrase, which comprises three His residues and is now believed¹¹ not to be affected by the replacement with a Cd^{2+} ion. Perhaps having more or different ligands bound to the metal is necessary to understand the toxicological affects of the cadmium ion and to better mimic its other biological states (e.g., zinc fingers where the metal is complexed by one or two histidine residues in addition to two or three cysteines). Future work could include the addition of solvent molecules like water or methanol, using less complicated amino acids like cysteine (to avoid the side chain affects on the spectra seen here), or including more amino acids as typically found physiologically [e.g., $Zn^{2+}(His)_2(Cys)_2$].

■ ASSOCIATED CONTENT

Supporting Information. Additional information as discussed in the text. This material is available free of charge via the Internet at <http://pubs.acs.org>.

■ AUTHOR INFORMATION

Corresponding Author

*E-mail: armentrout@chem.utah.edu.

■ ACKNOWLEDGMENT

This work is part of the research program of FOM, which is financially supported by the Nederlandse Organisatie voor Wetenschappelijk Onderzoek (NWO). Additional financial assistance was provided by the National Science Foundation, Grants No. CHE-1049580 and PIRE-0730072. In addition, the skilled assistance of the FELIX staff is gratefully acknowledged. Finally, we thank the Center for High Performance Computing at the University of Utah for their generous allocation of computer time, the use of which increased greatly during the various calculations on these large dimer complexes.

■ REFERENCES

- Pavletich, N. P.; Pabo, C. O. *Science* **1991**, 809.
- Fairall, L.; Schwabe, J. W. R.; Chapman, L.; Finch, J. T.; Rhodes, D. *Nature* **1993**, 366, 483.
- Berg, J. M.; Shi, Y. *Science* **1996**, 271, 1081.
- Mackay, J. P.; Crossley, M. *Trends Biochem. Sci.* **1998**, 23, 1.
- Iuchi, S.; Kuldell, N. *Zinc Finger Proteins from Atomic Contact to Cellular Function*; Kluwer Academic/Plenum Publishers: New York, 2005.
- Spiro, T. G. *Zinc Enzymes*; Wiley: New York, 1983.
- Hartwig, A.; Asmuss, M.; Blessing, H.; Hoffmann, S.; Jahnke, G.; Khandelwal, S.; Pelzer, A.; Burkle, A. *Food Chem. Toxicol.* **2002**, 40, 1179.
- Asmuss, M.; Mullenders, L. H. F.; Eker, A.; Hartwig, A. *Carcinogenesis* **2000**, 21, 2097.
- Salomons, W.; Förstner, U.; Mader, P. *Heavy Metals: Problems and Solutions*; Springer-Verlag: New York, 1995.
- Fergusson, J. E. *The Heavy Elements: Chemistry, Environmental Impact, and Health Effects*, 1st ed.; Pergamon Press: New York, 1990.
- Price, N. M.; Morel, F. M. M. *Nature* **1990**, 344, 658.
- Predki, P. F.; Sarkar, B. *J. Biol. Chem.* **1992**, 267, 5842.
- Berezovskaya, Y.; Armstrong, C. T.; Boyle, A. L.; Porrini, M.; Woolfson, D.; Barran, P. E. *Chem. Commun.* **2011**, 47, 412.
- Polfer, N. C.; Oomens, J.; Moore, D. T.; von Helden, G.; Meijer, G.; Dunbar, R. C. *J. Am. Chem. Soc.* **2006**, 128, 517.
- Dunbar, R. C.; Hopkinson, A. C.; Oomens, J.; Siu, C. K.; Siu, K. W. M.; Steill, J. D.; Verkerk, U. H.; Zhao, J. F. *J. Phys. Chem. B* **2009**, 113, 10403.
- Citir, M.; Hinton, C. S.; Oomens, J.; Steill, J. D.; Armentrout, P. B. *J. Phys. Chem. A*, submitted for publication.
- Kimura, E. *Acc. Chem. Res.* **2001**, 34, 171.
- Marino, T.; Russo, N.; Toscano, M. *J. Am. Chem. Soc.* **2005**, 127, 4242.
- Dunbar, R. C.; Steill, J. D.; Polfer, N. C.; Oomens, J. *J. Phys. Chem. A* **2009**, 113, 845.
- Prell, J. S.; O'Brien, J. T.; Steill, J. D.; Oomens, J.; Williams, E. R. *J. Am. Chem. Soc.* **2009**, 131, 11442.
- O'Brien, J. T.; Prell, J. S.; Berden, G.; Oomens, J.; Williams, E. R. *Int. J. Mass Spectrom.* **2010**, 297, 116.
- Dunbar, R. C.; Polfer, N. C.; Oomens, J. *J. Am. Chem. Soc.* **2007**, 129, 14562.
- Sousa, S. F.; Fernandes, P. A.; Ramos, M. J. *J. Am. Chem. Soc.* **2007**, 129, 1378.
- Duchackova, L.; Steinmetz, V.; Lemaire, J.; Roithova, J. *Inorg. Chem.* **2010**, 49, 8897.
- Duchackova, L.; Schroder, D.; Roithova, J. *Inorg. Chem.* **2011**, 50, 3153.
- Valle, J. J.; Eyler, J. R.; Oomens, J.; Moore, D. T.; van der Meer, A. F. G.; von Helden, G.; Meijer, G.; Hendrickson, C. L.; Marshall, A. G.; Blakney, G. T. *Rev. Sci. Instrum.* **2005**, 76, 023103.
- Polfer, N. C.; Oomens, J. *Phys. Chem. Chem. Phys.* **2007**, 9, 3804.
- Oepts, D.; van der Meer, A. F. G.; van Amersfoort, P. W. *Infrared Phys. Technol.* **1995**, 36, 297.
- Frisch, M. J.; Trucks, G. W.; Schlegel, H. B.; Scuseria, G. E.; Robb, M. A.; Cheeseman, J. R.; Scalmani, G.; Barone, V.; Mennucci, B.; Petersson, G. A.; Nakatsuji, H.; Caricato, M.; Li, X.; Hratchian, H. P.; Izmaylov, A. F.; Bloino, J.; Zheng, G.; Sonnenberg, J. L.; Hada, M.; Ehara, M.; Toyota, K.; Fukuda, R.; Hasegawa, J.; Ishida, M.; Nakajima, T.; Honda, Y.; Kitao, O.; Nakai, H.; Vreven, T.; Montgomery, J., J. A.; Peralta, J. E.; Ogliaro, F.; Bearpark, M.; Heyd, J. J.; Brothers, E.; Kudin, K. N.; Staroverov, V. N.; Kobayashi, R.; Normand, J.; Raghavachari, K.; Rendell, A.; Burant, J. C.; Millam, J. M.; Iyengar, S. S.; Tomasi, J.; Cossi, M.; Rega, N.; Millam, J. M.; Klene, M.; Knox, J. E.; Cross, J. B.; Bakken, V.; Adamo, C.; Jaramillo, J.; Gomperts, R.; Stratmann, R. E.; Yazyev, O.; Austin, A. J.; Cammi, R.; Pomelli, C.; Ochterski, J. W.; Martin, R. L.; Morokuma, K.; Zakrzewski, V. G.; Voth, G. A.; Salvador, P.; Dannenberg, J. J.; Dapprich, S.; Daniels, A. D.; Farkas, O.; Foresman, J. B.; Ortiz, J. V.; Cioslowski, J.; Fox, D. J. *Gaussian 09, Revision A.02*; Gaussian Inc.: Pittsburgh, PA, 2009.
- Becke, A. D. *J. Chem. Phys.* **1993**, 98, 5648.
- Ditchfield, R.; Hehre, W. J.; Pople, J. A. *J. Chem. Phys.* **1971**, 54, 724.
- Weigend, F.; Ahlrichs, R. *Phys. Chem. Chem. Phys.* **2005**, 7, 3297.
- Andrae, D.; Haeussermann, U.; Dolg, M.; Stoll, H.; Preuss, H. *Theo. Chem. Acc.* **1990**, 77, 123.
- Schuchardt, K. L.; Didier, B. T.; Elsethagen, T.; Sun, L. S.; Gurumoorthi, V.; Chase, J.; Li, J.; Windus, T. L. *J. Chem. Inf. Model.* **2007**, 47, 1045.
- Perdew, J. P. *Phys. Rev. B* **1986**, 33, 8822.
- Möller, C.; Plesset, M. S. *Phys. Rev.* **1934**, 46, 618.
- Bauschlicher, C. W., Jr.; Maitre, P. J. *J. Phys. Chem.* **1995**, 99, 3444.

- (38) Heaton, A. L.; Bowman, V. N.; Oomens, J.; Steill, J. D.; Armentrout, P. B. *J. Phys. Chem. A* **2009**, *113*, 5519.
- (39) Citir, M.; Stennett, E. M. S.; Oomens, J.; Steill, J. D.; Rodgers, M. T.; Armentrout, P. B. *Int. J. Mass Spectrom.* **2010**, *297*, 9.
- (40) Carl, D. R.; Cooper, T. E.; Oomens, J.; Steill, J. D.; Armentrout, P. B. *Phys. Chem. Chem. Phys.* **2010**, *12*, 3384.
- (41) Wilson, R. G.; Brewer, G. R. *Ion Beams with Applications to Ion Implantation*; Wiley: New York, 1973.
- (42) Armentrout, P. B.; Rodgers, M. T.; Oomens, J.; Steill, J. D. *J. Phys. Chem. A* **2008**, *112*, 2248.
- (43) Rodgers, M. T.; Armentrout, P. B.; Oomens, J.; Steill, J. D. *J. Phys. Chem. A* **2008**, *112*, 2258.
- (44) Oomens, J. M., D.T.; Meijer, G.; von Helden, G. *Phys. Chem. Chem. Phys.* **2004**, *6*, 710.
- (45) Sinclair, W. E.; Pratt, D. W. *J. Chem. Phys.* **1996**, *105*, 7942.
- (46) Carlson, R. H.; Brown, T. L. *Inorg. Chem.* **1966**, *5*, 208.
- (47) Cordes, M. d. N. D.; Walter, J. L. *Spectrochim. Acta* **1968**, *24A*, 237.